OPEN ACCESS Freely available online

PLOS ONE

Schisandra chinensis Peptidoglycan-Assisted Transmembrane Transport of Lignans Uniquely Altered the Pharmacokinetic and Pharmacodynamic Mechanisms in Human HepG2 Cell Model

Charng-Cherng Chyau[1], Yaw-Bee Ker[2], Chi-Huang Chang[1], Shiau-Huei Huang[1], Hui-Er Wang[2], Chiung-Chi Peng[3]*, Robert Y. Peng[1,4]*

1 Research Institute of Biotechnology, Hungkuang University, Shalu County, Taichung City, Taiwan, **2** Department of Food And Applied Technology, Hungkuang University, Shalu County, Taichung City, Taiwan, **3** Graduate Institute of Clinical Medicine, Taipei Medical University, Taipei, Taiwan, **4** Research Institute of Medical Sciences, Taipei Medical University, Taipei, Taiwan

Abstract

Schisandra chinensis (Turz Baill) (*S. chinensis*) (SC) fruit is a hepatoprotective herb containing many lignans and a large amount of polysaccharides. A novel polysaccharide (called SC-2) was isolated from SC of MW 841 kDa, which exhibited a protein-to-polysaccharide ratio of 0.4089, and showed a characteristic FTIR spectrum of a peptidoglycan. Powder X-ray diffraction revealed microcrystalline structures within SC-2. SC-2 contained 10 monosaccharides and 15 amino acids (essential amino acids of 78.12%w/w). In a HepG2 cell model, SC-2 was shown by MTT and TUNEL assay to be completely non-cytotoxic. A kinetic analysis and fluorescence-labeling technique revealed no intracellular disposition of SC-2. Combined treatment of lignans with SC-2 enhanced the intracellular transport of schisandrin B and deoxyschisandrin but decreased that of gomisin C, resulting in alteration of cell-killing bioactivity. The Second Law of Thermodynamics allows this type of unidirectional transport. Conclusively, SC-2 alters the transport and cell killing capability by a ''Catcher-Pitcher Unidirectional Transport Mechanism''.

Citation: Chyau C-C, Ker Y-B, Chang C-H, Huang S-H, Wang H-E, et al. (2014) *Schisandra chinensis* Peptidoglycan-Assisted Transmembrane Transport of Lignans Uniquely Altered the Pharmacokinetic and Pharmacodynamic Mechanisms in Human HepG2 Cell Model. PLoS ONE 9(1): e85165. doi:10.1371/journal.pone.0085165

Editor: Alberto G. Passi, University of Insubria, Italy

Received June 6, 2013; **Accepted** November 23, 2013; **Published** January 27, 2014

Funding: This study was supported by grants from the National Science Council of Taiwan (NSC-97-2313-B-241-002-MY3 and NSC-100-2313-B-241-004). Additional support was received from Taipei Medical University (TMU101-AE1-B11 and TMU102-SHH-11). The funders had no role in study design, data collection and analysis, decision to publish, or preparation of the manuscript.

Competing Interests: The authors have declared that no competing interests exist.

* E-mail: misspeng@ms2.hinet.net (CCP); ypeng@seed.net.tw (RYP)

Introduction

The primary function of polysaccharides is supposed only to assist tissue hydration and increase tissue resilience [1,2]. Pharmaceutically, polysaccharides exhibit a diversity of uses including the drug transport improver [3], sustaining medicine transport [4], serving as an anchorage site for drug delivery liposomes [5], and enhancing the water solubility of carotenoids [6]. Hyaluronan, which was originally determined to act as intercellular glue, was recently found to be a very potent intracellular signaling agent associated with multiple drug resistance [2], immunity and oncology [7,8].

Schisandra chinensis Turz Baill of the Magnoliaceae (*Wuweizi* in Chinese) (SC) is widely used as a valuable phytomedicine in China, Korea, and Japan to treat dysfunctional livers, lungs, hearts, and kidneys [9] and for chemical/viral hepatitis [10,11]. Dibenzocyclooctadiene lignans isolated from SC (abbreviated as SCLs) include schizandrin, deoxyschisandrin (schisandrin A, SA), gomisins, schisandrol B, γ-schisandrin, wuweizisu B and C, and schisantherin C [12]. It is worth noting that the lignan compositional profile may depend on the separation technology [13].

Recently, SCLs like SA, Schisandrin B (SB) and gomisin C (GmC) have been well indicated to exhibit potent hepatoprotectives, anti-inflammatory, anticarcinogenics, antiviral, anti-HIV, immunomodulaters, and antioxidative properties [9,11,14–19]. By inhibiting P4503A4 activity, schisandrol A and gomisin A were shown to affect cellular drug metabolism and uptake. Biological studies indicated that an extract of SC seeds enhanced the hepatic glutathione (GSH) antioxidant/detoxification system and facilitated both processes in the livers, consequently considered to be a promising agent for improving phase I oxidative metabolism in CCl_4-damaged livers [20]. Moreover, compound SB+sesamin preparation reveals a prominent *in vivo* hepatoprotective effect [21].

Recently, the bioactivity of soluble polysaccharide of *Schisandra* fruits was found to have potent immunomodulating properties, like improving the weight of immune organs and enhancing the phagocytic activity of peritoneal macrophages [22]. Yan et al. demonstrated a rather promising synergistic hepatoprotective effect of SCLs when co-administered with *Astragalus* polysaccharides [23]. Previously, we found the peptidoglycan (named SC-2) to be biologically inactive against the HepG2 cells (unpublished

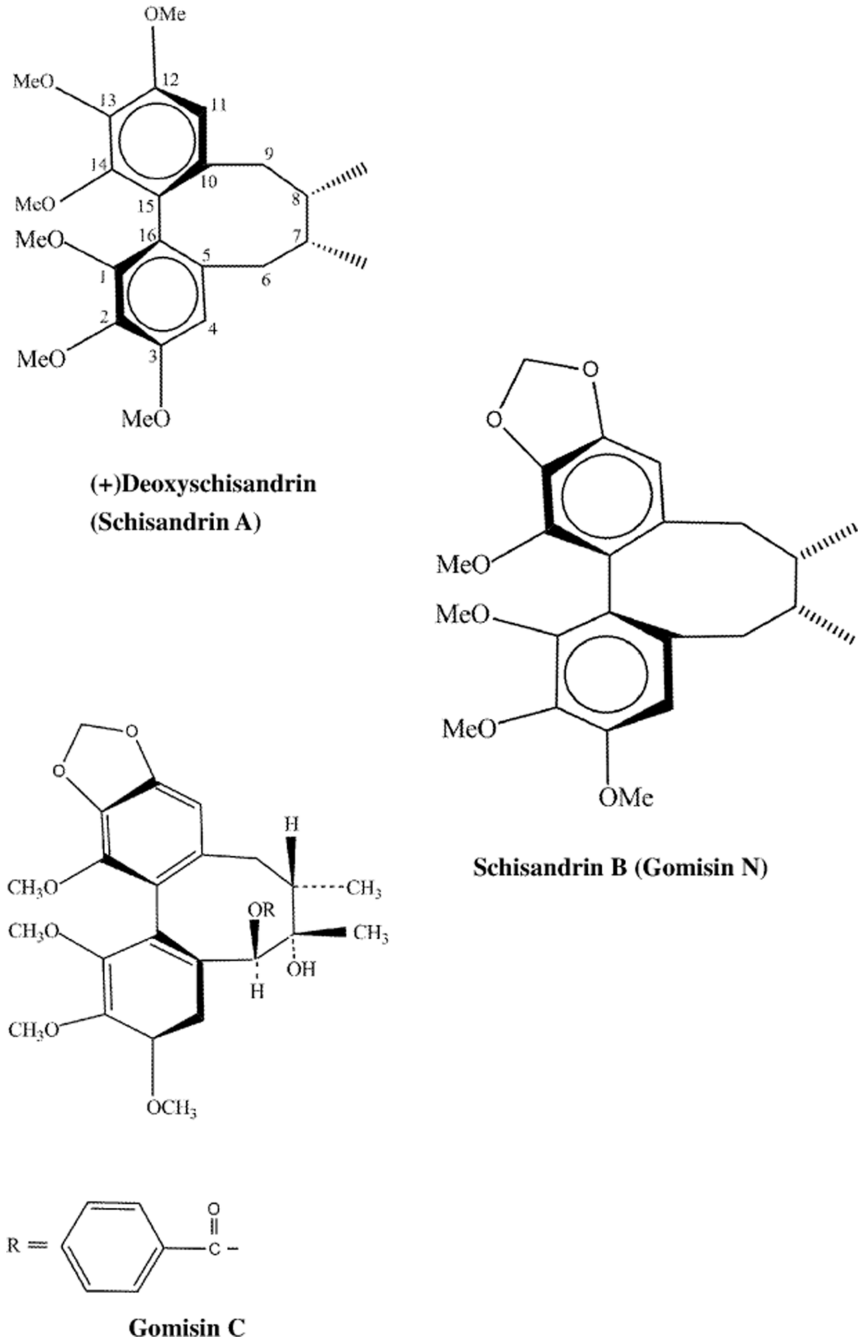

Figure 1. Chemical structures of liganas isolated from *S. chinensis* fruits. Gomisin C, deoxyschisandrin and schisandrin B isolated from the *S. chinensis* fruits. Structures of (+)deoxyschisandrin and (−)schisandrin B are depicted from Gnabre et al. (2010) [27]. Structure of gomisin C is depicted from Wang et al, (1994) [36].
doi:10.1371/journal.pone.0085165.g001

data). However, since SC-2 is water soluble in nature and decoction process has been always preferred for many Chinese Medicinal Preparations, we hypothesize that SC-2 with certain unknown mechanism might favor the therapeutic effect of SCLs. To verify this, the therapeutic effect of a serial model of SC-2, either used alone or in combination with individual SCLs, was extensively explored.

Materials and Methods

Isolation and purification of dibenzocyclooctadiene lignans

Desiccated sample SC fruits were purchased from Sun Ten Pharmaceutical Corp. (Taipei, Taiwan, ROC). Ten grams of desiccated fruits were extracted three times with 95% ethanol; each time 100 ml was extracted for 30 min in a sonication-assisted extractor. We have described the detailed methods in Text S1.

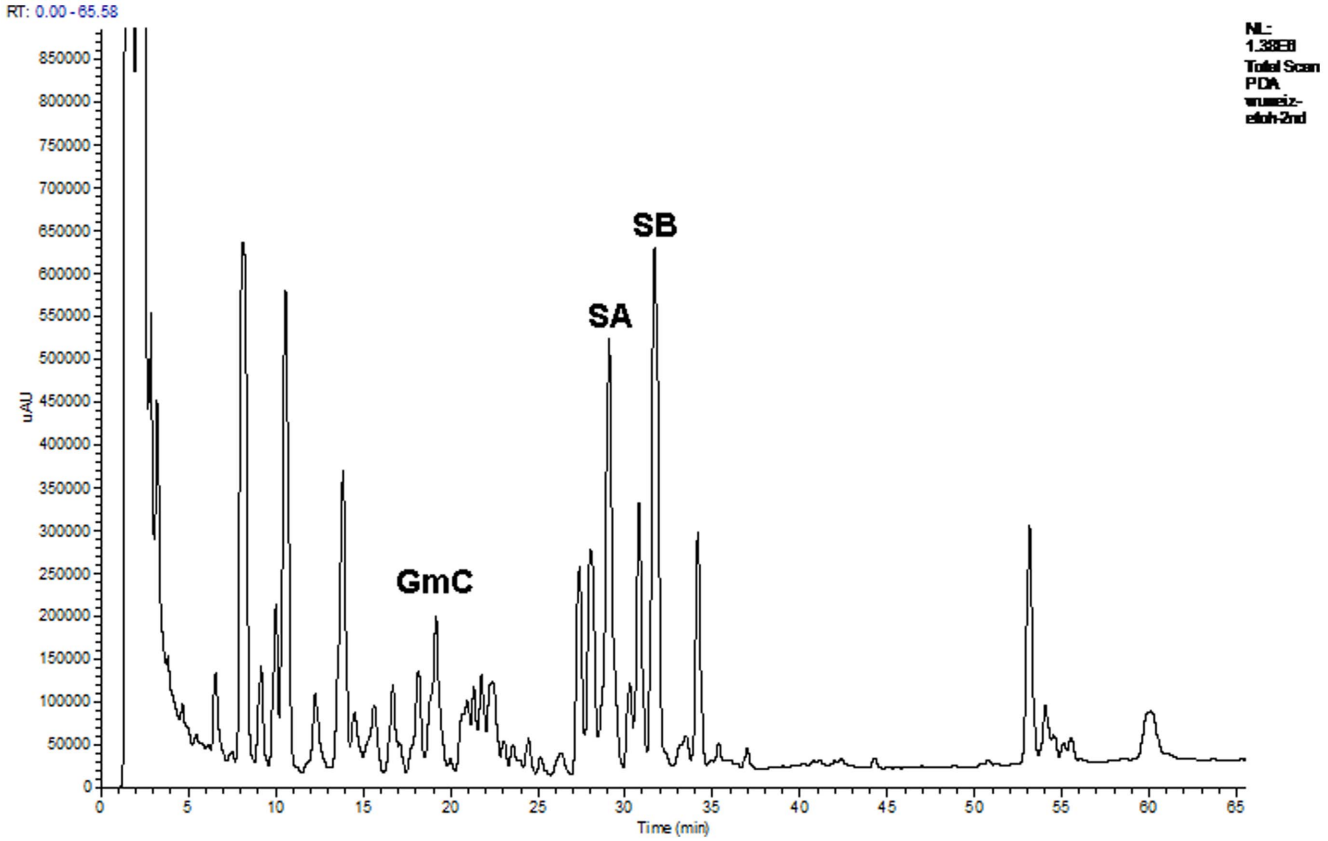

Figure 2. Spectral characterization of the peptidoglycan SC-2 isolated a from *S. chinensis* fruits. The absorption at 490 nm determines the carbohydrate content and the absorption at 280 nm measures the peptide content (A). Purity identification of SC-2 obtained from the fractions 33–39 obtained by Sephadex G-100 column by high-performance size exclusion chromatography (HPSEC) with a PolySep GFC P-4000 column (300×7.8 mm) with water as eluant at a flow rate of 0.8 ml/min (B). The FTIR spectrum of purified SC-2. C (C): And the X-ray powder diffraction pattern of SC-2 (D).
doi:10.1371/journal.pone.0085165.g002

High-performance liquid chromatographic (HPLC)/ electrospray ionization (ESI)/tandem mass spectrometry (MS/MS) analyses

Separation of the dibenzocyclooctadiene lignans was conducted on a Luna C18(2) column ($\ell \times$i.d. = 2.00×150 mm, thickness = 3.0 μm) and a guard column ($\ell \times$id = 10×3 mm, Phenomenex Inc., Torrance, CA., U.S.A.) using an HPLC system consisting of a Finnigan Surveyor module separation system and a photodiode-array (PDA) detector (Thermo Electron Co., MA., U.S.A.). The next elution process and instrument setting was carried out according to La Torre et al. [24]. We have described the detailed methods in Text S1.

Fourier transform infrared (FTIR) analyses of isolated lignans

The lignans SA, SB and GmC were separately desiccated under a vacuum at 40°C for 16 h, respectively mixed with KBr powder (IR grade) at a ratio lignan: KBr = 1: 100 (w/w) and fabricated into tablets. The tablet was scanned with Shimazdu 8400S FTIR 460 (Shimadzu, Tokyo, Japan) spectrophotometer against the KBr blank at 400~4000 cm^{-1} and a resolution of 2 cm^{-1}. Each sample was repeatedly scanned at least 10 times to assure the precision of the data. We have described the detailed methods in Text S1.

Solvent extraction of crude polysaccharides from SC

The method for extraction of crude polysaccharides from SC (SC-CP) was carried out according to Ker et al. [25]. We have described the detailed methods in Text S1.

Purification of crude polysaccharides from SC

Further isolation and purification of SC-CP were conducted with gel permeation chromatography (GPC) carried out according to Ker et al. [25] (be referred to Text S1). The yield of the purified product of the second fraction of SC-polysaccharide was 3.58%w/w (denoted as SC-2). We have described the detailed methods in Text S1 [26,31].

Characterization of the molecular weight and the molar extinction coefficient with high-performance size exclusion chromatography-tandem UV-visible and evaporative light scattering detection (HPSEC-UV-ELSD)

The HPSEC-UV-ELSD analysis was conducted to determine the molecular weight of SC-2. We have described the detailed methods in Text S1.

X-ray powder diffraction (powder XRD) of SC-2

Desiccated purified SC-2 powder was macerated to fine, homogenous consistency and subjected to an X-Ray diffraction

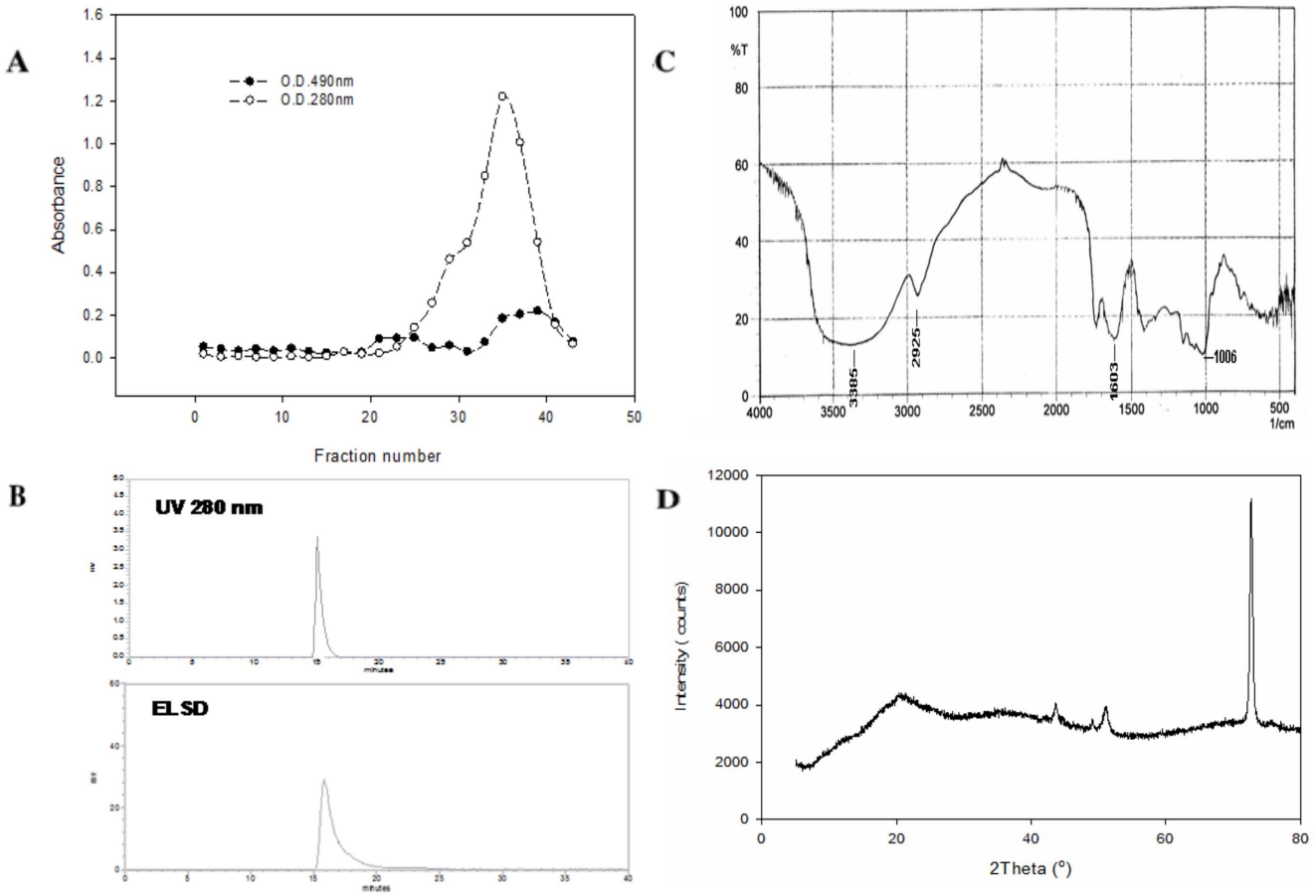

Figure 3. HPLC chromatographic analysis of the ethanolic extract of *S. chinensis* fruits. The retention times for the dibenzocyclooctadiene lignans were: gomisin C (GmC), 19.17 min; deoxyschisandrin (SA), 29.07 min; schisandrin B (SB), 31.69 min; gomisin O, 8.13 min; schizandrol B, 10.56 min; and gomisin R, 13.85 min, respectively.
doi:10.1371/journal.pone.0085165.g003

analyzer (X'Pert Pro MRD, PANalytical B. V., Almelo, The Netherlands). We have described the detailed methods in Text S1.

FTIR analyses of purified SC-2 and pure lignans+SC-2

To measure the combined IR spectra, pure SC-2 alone was used as reference blank. The other combined formula were prepared by mixing each lignans with SC-2 at equimolar ratio, i.e. for SA+SC-2: 2 mL of SA solution (1.04 mg in 25 mL)+2 mL of SC-2 solution (1 mg mL^{-1}). For SB+SC-2: 2 mL of SB (4 mg in 25 mL)+2 mL of SC-2 (4 mg mL^{-1}); and for GmC+SC-2: 2 mL of GmC solution (5.2 mg in 25 mL)+2 mL of SC-2 solution (4 mg mL^{-1}) were used. We have described the detailed methods in Text S1.

Monosaccharide composition of SC-2

The method for analyzing the monosaccharide composition was based on previous work [25,26]. We have described the detailed methods in Text S1 [25,35].

Amino acid composition in the protein moiety of SC-2

The method for analyzing the amino acid composition was according to previous work of Ker et al. [25]. We have described the detailed methods in Text S1 [25].

Source and cell line

The human hepatocellular carcinoma cell line, HepG2 (BCRC 60380), was obtained from the Bioresource Collection and Research Center (BCRC, Food Industry Research and Development Institute, Hsin-Chu City, Taiwan). The detailed methods for cultivation and stocking are described in Text S1.

Cell culture and cell viability assay

Cultivation of HepG2 cells and the MTT assay were performed as previously reported [27]. We have described the detailed methods in Text S1.

Determination of the uptake rate of free SB, GmC, and deoxyschisandrin in the absence and presence of SC-2 by HepG2 cells

We have described the detailed methods in Text S1.

Determination of the intracellular disposition of SC-2 in HepG2 cells

Fluorescein isothiocyanate (FITC) labeling of SC-2. Methods of Kanebo et al. [28] and Tanaka et al. [29] were followed with slight modification. We have described the detailed methods in Text S1.

Intracellular disposition of FITC-labeled SC-2. HepG2 cells (1×10^5 cells/mL) were seeded onto a 3.5 cm dish containing

Table 1. The compositional analysis of the glycoprotein SC-2 purified from *S. chinensis* fruits.

Overall yield of purified SC-2, %w/w		3.58	
Mean molecular weight, kDa		841	
Proximate analysis (%w/w/)			
Total carbohydrate content		68.97	
Crude protein content		28.20	
Monosaccharide and amino acid composition of SC-2			
monosaccharide	**Content (mol%)**	**Amino acid**	**Content (%w/w)**
Rhamnose	14.64	Alanine	0.18
Fucose	28.97	Glycine	0.40
Ribose	4.61	Valine	10.34
Arabinose	13.74	Leucine	15.80
Xylose	13.32	Isoleucine	14.29
Allose	8.34	Proline	0.09
Talose	2.13	Methionine	1.98
Mannose	1.84	Glutamic acid	0.38
Galactose	n.d	Hydroxyproline	1.96
Glucose	11.12	Phenylalanine	21.54
Myo-inositol	1.29	Cysteine	2.60
		Lysine	8.63
		Tyrosine	2.94
		Aspartic acid	1.72
		Histidine	17.15

n.d.: not detected.

doi:10.1371/journal.pone.0085165.t001

2 mL of DMEM medium. After incubated for 24 h at 37°C, FITC-SC-2 at 0.01, 0.1, 1.0, 10.0, and 25 μg mL^{-1} were added and incubated to investigate the dose- and time–dependent effects on the disposition of SC-2. We have described the detailed method in Text S1 [28,29].

Terminal deoxynucleotidyl transferase-mediated dUTP nick end-labeling (TUNEL) assay

A TUNEL assay using the Fluorescein Apoptosis Detection Kits (Roche Applied Science, Indianapolis, IN, USA) was carried out according to the manufacturer's instructions by Borisov et al. [30]. We described the detailed methods in Text S1 [31].

Statistical analysis

Data obtained in the same group were analyzed by an analysis of variance (ANOVA) and Student's *t*-test with computer statistical software SPSS 10.0 (SPSS, Chicago, IL, USA). Statistical Analysis System (2000) software was used to analyze the variances, and Duncan's multiple-range test was used to test the significance of difference between paired means. The significance of the difference was judged by a confidence level of $p<0.05$.

Results

HPLC and ESI/MS/MS analysis of GmC Deoxyschisandrin (SA) and SB

The retention times of GmC, SA and SB (Fig. 1) in HPLC were 19.17, 29.07 and 31.69 min (Fig. 2) and their molecular weights were 536.6, 416.5 and 400.5, respectively (Fig. S1).

Characterization of SC-2

The purified soluble polysaccharide, named hereafter SC-2, showed an overall yield 3.58% (Fig. 3A, Table 1). SC-2 exhibited a MW 841 kDa (Fig. 3B) and molar extinctions 1.0260×10^7 M^{-1} and 1.766×10^7 M^{-1} at 280 nm and 490 nm, respectively (Fig. 3A). It contained 28.20 wt% protein and 68.97 wt% carbohydrate, yielding a ratio protein/carbohydrate = 0.4089 (Table 1). The sugar portion of SC-2 contained 10 monosaccharide species (Table 1). Their contents (in mol%) were fucose (28.64), rhamnose (14.64), arabinose (13.74), xylose (13.32), glucose (11.12), allose (8.34), ribose (4.61), talose (2.13), mannose (1.84) and myoinsitol (1.29) respectively, but galactose was completely absent (Table 1). SC-2 comprised 15 kinds of amino acids. The major ten were (in %w/w): valine (10.34), leucine (15.80), isoleucine (14.29), methionine (1.98), proline (0.09)+hydroxyproline (1.96) (= 2.05), phenylalanine (21.54)+tyrosine (2.94) (= 24.48), cysteine (8.63), and histidine (17.15). The total essential amino acids amounted to 80.3%w/w (Table 1). The FTIR (KBr) ν_{max} (cm^{-1}): spectrum showed many characteristic absorption bands, such as 3384.91 ($\nu_{O\text{-}H}$, s, broad, polyhydroxyl hydrogen bonding), 3144.07, 3087.17 (aromatic $\nu_{C\text{-}H}$, s), 2857.64 ($\nu_{C\text{-}H}$, CH_3, m), 1734.17 ($\nu_{C=O}$, m), 1647.02 ($\nu_{C=O}$, amide, s), 1602.9, 1457.27 ($\delta_{N\text{-}H}$, amide, s), 1339.61 ($\nu_{C\text{-}O}$, amide, m), 1151.54 ($\nu_{C\text{-}O}$, alcohol, s), 1100~1010 ($\nu_{C\text{-}O}$, β-pyranoside, s), 1075.35 ($\nu_{C\text{-}O}$, ester, s), 1006.88 ($\nu_{C\text{-}O}$, ether, s), 952.87, 854.49 ($\delta_{C\text{-}H}$, alkene, s), 768.66, 761.78 ($\delta_{C\text{-}O}$, β-glycosidic linkage, w) and 680–760 ($\delta_{C\text{-}H}$, aromatic, s)(Fig. 3C).

The powder XRD pattern revealed three 2θ peaks, i.e. $2\theta_1 = 42.2160°$ with an intensity of 3644; $2\theta_2 = 51.1398°$ with an intensity of 3938; and $2\theta_3 = 72.66393°$ with intensity of 11190,

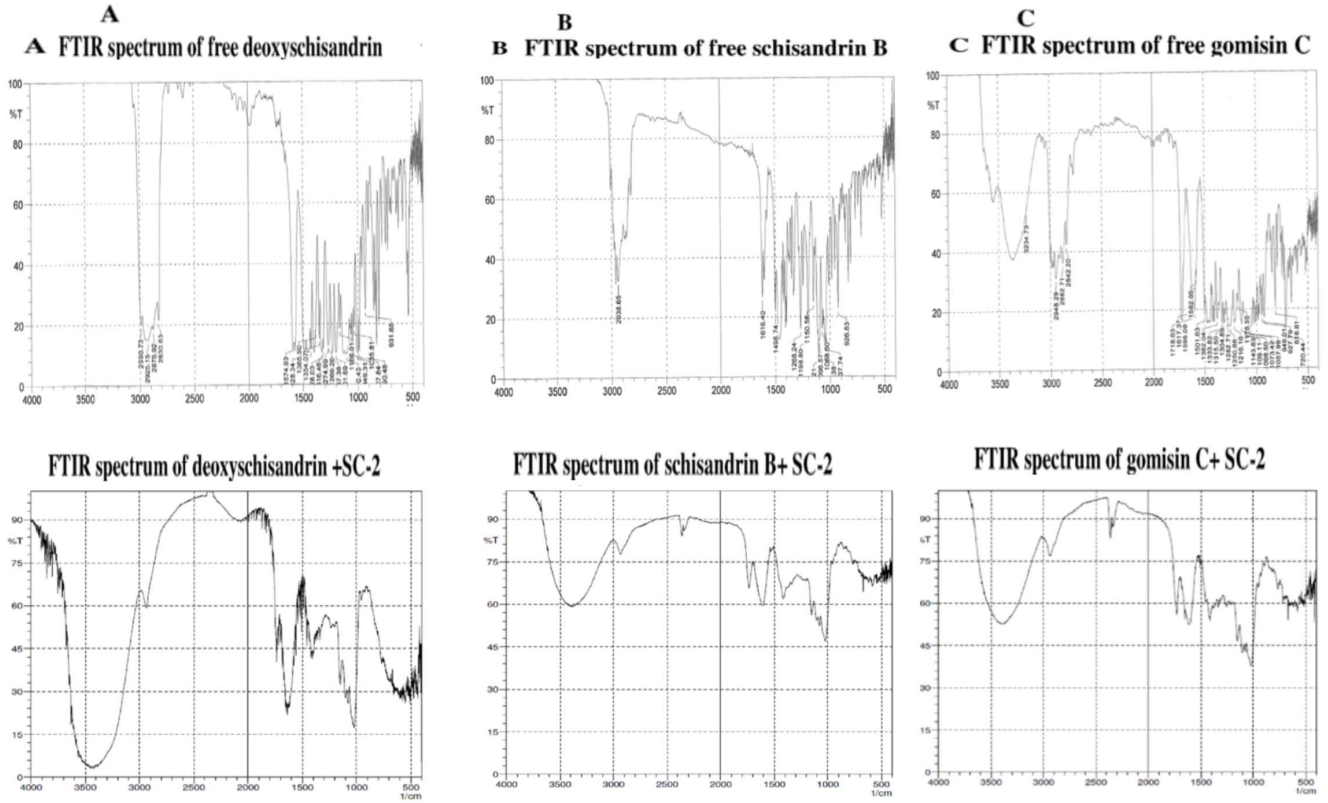

Figure 4. FTIR spectra of the purified free lignans and the lignans+SC-2. Purified free deoxyschisandrin (upper panel) and deoxyschsandrin+SC-2 (lower panel) (A). Purified free schisandrin B (upper panel) and schisandrin B+SC-2 (lower panel) (B). And purified free gomisin C (upper panel) and gomosin C+SC-2 (lower panel) (C). In measuring of the combined IR spectra, equimolar amount of each was used: for deoxyschisandrin+SC-2: 2 mL of deoxyschisandrin solution (1.04 mg/25 mL)+2 mL of SC-2 solution (1 mg/mL). For schisandrin B+SC-2: 2 mL of schisandrin B (4 mg/25 mL)+2 mL of SC-2 (4 mg/mL). And for gomisin C+SC-2: 2 mL of gomisin solution (5.2 mg/25 mL)+2 mL of SC-2 solution (4 mg/mL) were used. The mixture was respectively mixed thoroughly with KBr (IR grade) (in 1:100 w/w), dried at 40°C under vacuum for 16 h, fabricated into KBr tablets and subjected to FTIR scanning using Shimadzu FTIR 460 (Shimadzu, Tokyo, Japan). Each sample was repeatedly scanned for at least 10 times to assure the precision of the data.
doi:10.1371/journal.pone.0085165.g004

giving the specific diffraction angles at $\theta_1 = 21.1080°$, $\theta_2 = 25.5699°$, and $\theta_3 = 36.3319°$, respectively (Fig. 3D).

FTIR and UV-Vis- ESI-MS- ESI-MS-MS characterization of the isolated lignans

For free SA: UV λ_{max} (nm): 234, 254 (sh); ESI(+)-MS (m/z): 417 $[M+H]^+$ (Fig. S1).

IR (KBr) ν_{max} (cm^{-1}): 2990.73, 2925.15, 2876.92, 2830.63 ($\nu_{C\text{-}H}$, CH_3, s), 1574.93, 1428.34, 1385.90, 1354.07, 1328.03, 1316.46, 1274.99, 1269.20, 1201.69 ($\nu_{C\text{-}O}$, phenolic, s), 1166.01, 1100.43, 1049.31, 1035.81, 1007.84 ($\nu_{C\text{-}O}$, etheric, s), 990.48, 931.65 ($\delta_{C\text{-}H}$, s, 2 peaks) (Fig. 4A, upper panel).

For free SB: UV λ_{max} (nm): 237, 262 (sh); ESI(+)-MS (m/z): 401 $[M+H]^+$ (Fig. S1).

IR (KBr) ν_{max} (cm^{-1}): 2970.00, 2938.38, 2830.00 ($\nu_{C\text{-}H}$, CH_3, s), 1616.4 (aromatic $\nu_{C\text{-}H}$, s), 1498.74, 1268.24 (phenolic $\nu_{C\text{-}O}$, s), 1198.80, 1150.58, 1106.21, 1096.57, 1068.60, 1047.38, 1037.74 (etheric $\nu_{C\text{-}O}$, s), 926.83, 937.22 ($\delta_{C\text{-}H}$, s, 2 peaks) (Fig. 4B, upper panel).

For free GmC: UV λ_{max} (nm): 236, 258 (sh); ESI(+)-MS (m/z): 537 $[M+H]^+$ (Fig. S1). IR (KBr) ν_{max} (cm^{-1}): 3600.00 ($\nu_{O\text{-}H}$, alcohol s), 3234.73 ($\nu_{O\text{-}H}$, phenolic s, m broad H-bonding), 2948.29, 2882.71, 2842.20 ($\nu_{C\text{-}H}$, s), 1718.63 ($\nu_{C=O}$, s), 1617.37, 1598.08, 1582.65, 1501.63 ($\nu_{C=C}$, aromatic, s), 1382.04, 1333.82 ($\nu_{O\text{-}H}$, phenolic, s, 2 peaks), 1282.71, 1250.88, 1216.16, 1178.55, 1143.83, 1109.11, 1098.50, 1073.42, 1057.99 ($\nu_{C\text{-}O}$, etheric, s), 949.01, 927.79 ($\delta_{C\text{-}H}$, alkene, s), 818.81 ($\delta_{C\text{-}H}$, polysubstituted aromatic, s) and 720.44 ($\delta_{C\text{-}H}$, C6-monosubstituted aromatic, s) (Fig. 4C, upper panel).

FTIR spectra of the combined lignans plus SC-2

Surprisingly, we found the FTIR spectra of the combined lignans+SC-2 (Fig. 4) to be rather similar to that of SC-2 (Fig. 2C) alone.

For SA+SC-2, IR (KBr) ν_{max} (cm^{-1}): 3384.92 ($\nu_{O\text{-}H}$, s, broad, polyhydroxyl hydrogen bonding), 2925.15 ($\nu_{C\text{-}H}$, CH_3O-, m), 1750 ($\nu_{C=O}$, esteric, s), 1608–1650, ($\nu_{C=O}$, amide, m) 1420 1400 ($\nu_{C\text{-}N}$, amide, m), 1360 ($\nu_{C\text{-}O}$, amide, m), 1200 ($\nu_{C\text{-}O}$, phenolic, s), 1150, 1105 ($\nu_{C\text{-}O}$, alcoholic, s), 1105, 1023 ($\nu_{C\text{-}O}$, β-pyranoside, s). 768.34, 761.28 ($\delta_{C\text{-}O}$, β-glycosidic linkage, w), 760–690 ($\delta_{C\text{-}H}$, aromatic, disappeared or masked by SC-2) (Fig. 4A, lower panel).

For SB+SC-2, IR (KBr) ν_{max} (cm^{-1}): 3400.30 ($\nu_{O\text{-}H}$, s, broad, polyhydroxyl hydrogen bonding), 2938.65 ($\nu_{C\text{-}H}$, CH_3O-, m), 2385.30, 2379.24 ($\nu_{C\text{-}H}$, -CH = N-, m), 1740.33 ($\nu_{C=O}$, s), 1615.80 ($\nu_{C\text{-}H}$, conjugated alkene, s), 1400.02 ($\nu_{C\text{-}N}$, amide, s), 1160.50, 1030.34 ($\nu_{C\text{-}O}$, ether, s), 760–690 ($\delta_{C\text{-}H}$, aromatic, disappeared or masked by SC-2) (Fig. 4B, lower panel).

For GmC+SC-2, IR (KBr) ν_{max} (cm^{-1}): 3485.26 ($\nu_{O\text{-}H}$, s, broad, polyhydroxyl hydrogen bonding), 2948.59 ($\nu_{C\text{-}H}$, CH_3O-, m), 2480.00, 2300.30 ($\nu_{C\text{-}H}$, -CH = N-, m), 1724.20 ($\nu_{C=O}$, esteric,

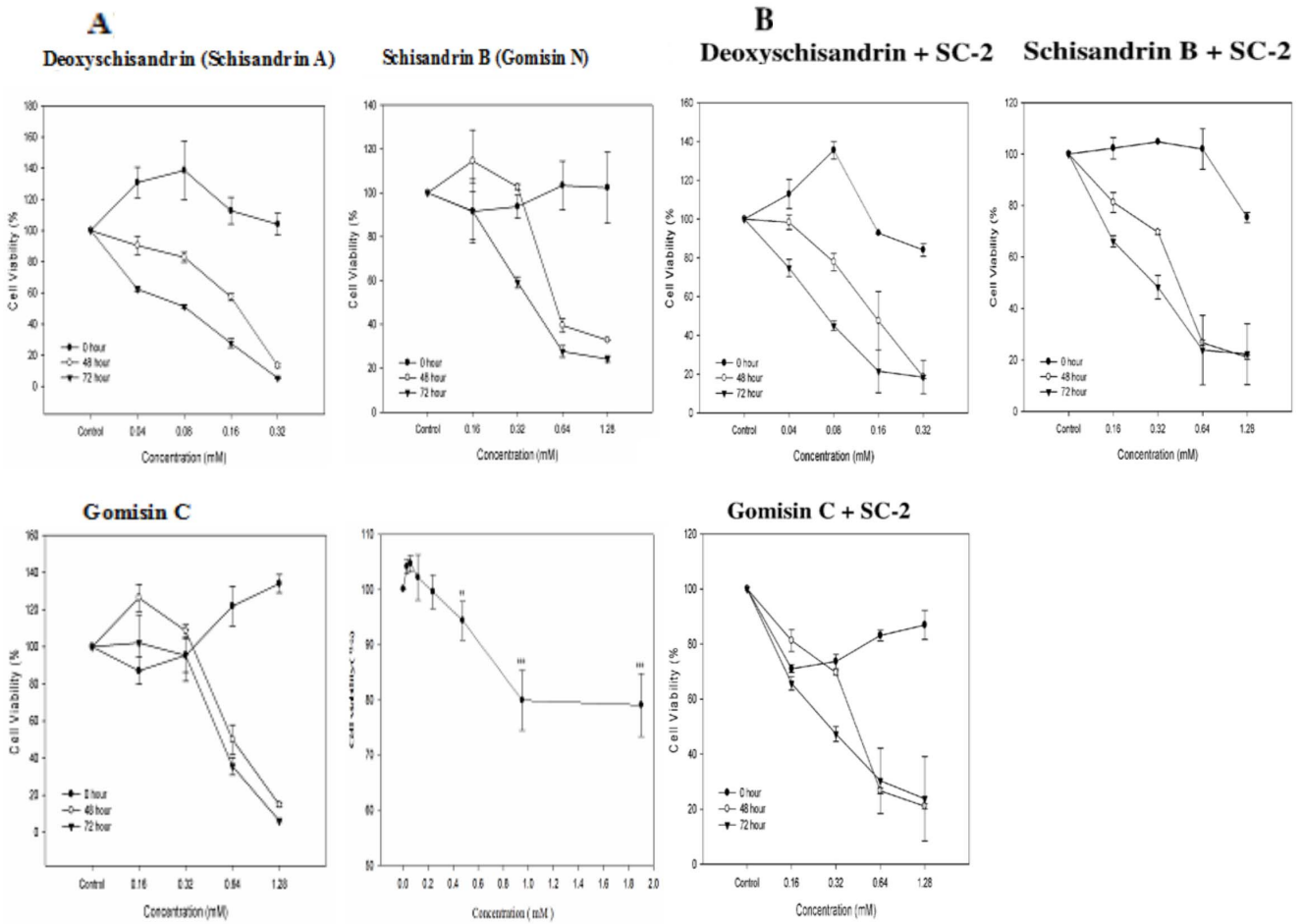

Figure 5. Effect of free lignans and the peptidylglycan SC-2 on HepG2 cell viability. The cell viability affected by the free lignans and SC-2 (A). And the cell viability affected by the combined therapy of ligna+SC-2 (B). For free SC-2 in figure 5A, the cells were cultured in 10% FBS medium and treated with SC-2 at dosages 0.0297 mM, 0.0595, 0.1189, 0.2378, 0.4756, 0.9512, and 1.9024 mM, respectively for 48 h. The percent cell viability was calculated by comparing with the control (arbitrarily set as 100%) Values are expressed as mean±S.D. of triplicate independent experiments (**$p<0.01$ and ***$p<0.001$ *vs* control group).
doi:10.1371/journal.pone.0085165.g005

s), 1612.20 ($\nu_{C=O}$, amide, s), 1425.00 ($\nu_{C\text{-}N}$, amide, s), 1160.11, ($\nu_{C\text{-}O}$, alcoholic, s), 1026.22 ($\nu_{C\text{-}O}$, etheric, s; $\nu_{C\text{-}O}$, β-pyranoside, s), 760–690 ($\delta_{C\text{-}H}$, aromatic, disappeared or masked by SC-2) (Fig. 4C, lower panel).

Effect of SC-2 on the cell viability of HepG2 cells

In medium containing 10% FBS, when treated with SC-2 at dosages 0.0297, 0.0595, 0.1189, 0.2378, 0.4756, 0.9512, and 1.9024 mM, respectively, the cell viability was seen still retaining at a level >80%, indicating the totally nontoxic behavior of SC-2 to HepG2 cells. At higher doses (0.9512~1.9024 mM), a slightly declined cell viability occurred, suggesting a masking or plugging effect of SC-2 on the cell membrane (Fig. 5D).

Pharmacokinetic behavior of lignans in HepG2 cells

The uptake rates of free *Shisandra* lignans by HepG2 cells greatly differed from those combined with SC-2. For SB and SA, the uptake rates were apparently elevated by presence of SC-2. On the contrary, GmC showed a lower uptake rate (Table 2).

Worth noting, free SA uniquely revealed a relatively delayed uptake rate that was totally not seen for the others (Table 2). In contrast, the uptake process was relatively shorter for both GmC and SA. Their peak points in uptake rates reached at or around 30 min (Table 2). Intracellular GmC was rapidly consumed up at 30 min for GmC and at 60 min for SA. The intracellular decay rate coefficient was $\sim 1.092\times10^{-6}$ L•mmol^{-1} min^{-1} for both GmC and SA (Table 2). A relatively longer uptake time was required by SB, which remained at 1.429×10^{-6} L•mmol^{-1} - min^{-1} even at 60 min (Table 2). The total amounts delivered from the extracellular to the intracellular compartments in the presence of SC-2 were (in decreasing order) SB>SA>GmC, corresponding to 91±5 μM (at 60 min)>77±5 μM (at 15 min)>19±3 μM (at 30 min), respectively. For comparison, the respective order of the free lignans was: 82±3, 63±6 and 27±1 μM. Interestingly, in the presence of SC-2 the uptake of GmC was significantly retarded (Table 2).

Pharmacodynamic behavior of lignans in HepG2 cells

Behaviors of HepG2 cells responding to these three lignans varied greatly depending on the dose, time of incubation, and the presence or absence of SC-2. At 48 h, free SB alone showed activated cell proliferation within doses of <0.16 mM (Fig. 5A). In the presence of SC-2, this activation disappeared (Fig. 5B). A similar phenomenon was seen for GmC (Fig. 5A & 5B), but not for

Table 2. Enhanced lignan uptake rate mediated by glycoprotein SC-2.

Incubation time, (min)	Schisandrin B		Schisandrin B+SC-2[a]	
	Uptake (μM)	Decay rate constant, k_1(min^{-1})	Uptake (μM)	Decay rate constant, k_2 ($L{\cdot}mmol^{-1}\ min^{-1}$)
0	47[b]	-	46[b]	-
5	54±2	0.0140[b]	58±2	2.016×10^{-5b}
15	68±3	0.0140	82±2**	2.016×10^{-5}
30	76±3	0.0053	86±4*	2.269×10^{-6}
60	82±3	0.0020	91±5	1.429×10^{-6}
90[b]	86[b]	0.0013[b]	93[b]	5.865×10^{-7b}
120[b]	82[b]	−00013[b]	89[b]	-1.092×10^{-6b}
Incubation time, (min)	**Gomisin C**		**Gomisin C+SC-2**	
	Uptake (μM)	Decay rate constant, k_1 (min^{-1})	Uptake (μM)	Decay rate constant, k_2 ($L{\cdot}mmol^{-1}\ min^{-1}$)
0	24[b]	-	10[b]	-
5	25±1	0.0020[b]	13±1**	5.046×10^{-6b}
15	27±3	0.0020	19±4*	5.046×10^{-6}
30	27±1	0.0000	19±3 *	0.0000
60	23±3	−0.1333	15±1	-1.092×10^{-6}
Incubation time, (min)	**Deoxyschisandrin**		**Deoxyschisandrin+SC-2**	
	Uptake (μM)	Decay rate constant, k_1 (min^{-1})	Uptake (μM)	Decay rate constant, k_2 ($L{\cdot}mmol^{-1}\ min^{-1}$)
0	43[b]	-	55[b]	-
5	48±2	0.0010[b]	62±0.4**	1.264×10^{-5b}
15	58±4	0.0010	77±5**	1.264×10^{-5}
30	63±6	0.0033	74±5	1.976×10^{-6}
60	59±2	−0.0013	70±2	-1.092×10^{-6}

[a]Dose of SC-2 (MW: 841 kDa): 1 mg/mL (=1.1891×10^{-3} mM) (*$p<0.05$; **$p<0.01$).
[b]Values obtained by extrapolation.
doi:10.1371/journal.pone.0085165.t002

SA (Fig. 5A & 5B). The IC_{50} values at 48 h were 0.55 mM, 0.64 mM and 0.19 mM without SC-2, while they significantly improved to 0.41. 0.51, and 0.15 mM, for SB, GmC and SA in the presence of SC-2, respectively (Table 3). Comparing to data at 48 h, the IC_{50} values at 72 h had further improved to 0.47 mM, 0.58 mM and 0.08 mM for the free lignans SB, GmC and SA (Table 3, Fig. 5A), and to 0.32 mM, 0.29 mM and 0.08 mM for SC-2+lignans, respectively (Table 3, Fig. 5B).

Table 3. The cytotoxicity and HepG2 cell killing-capability of dibenzocyclooctadiene lignans in the presence and absence of its coexisting glycoproteinSC-2[a].

Treatment	Incubation time, h			
	48		72	
	IC_{50}, mM	Killing capability, cells/mM[b]	IC_{50}, mM	Killing capability, cells/mM[b]
Schisandrin B	0.55±0.06	1.11×10^5 cells/mM (within 0.16–1.28 mM)	0.47±0.04	1.52×10^5 cells/mM (at <0.64 mM)
Schisandrin B+SC-2	0.41±0.03	1.82×10^5 cells/mM (at <0.64 mM)	0.30±0.14	1.76×10^5 cells/mM (at <0.64 mM)
Gomisin C	0.64±0.01	1.46×10^5 cells/mM (at >0.16 mM)	0.58±0.02	1.42×10^5 cells/mM (within 0.32–1.28 mM)
		1.73×10^5 cells/mM		
Gomisin C+SC-2	0.51±0.02	(at <0.64 mM; average of two phases)	0.29±0.04	3.94×10^5 cells/mM (at ≤1.28 mM)
Deoxyschisandrin	0.20±0.00	3.94×10^5 cells/mM(at <0.32 mM)	0.10±0.00	4.59×10^5 cells/mM (at <0.32 mM)
Deoxyschisandrin+SC-2	0.15±0.04	4.29×10^5 cells/mM(at <0.32 mM)	0.07±0.01	7.50×10^5 cells/mM (at <0.32 mM)

[a]Dose of SC-2 (MW: 841 kDa): 1 mg/mL (=1.1891×10^{-3} mM) (*$p<0.05$; **$p<0.01$).
[b]Killing capability was measured within the linearity range of viability-dose in Fig. 5A and 5B.
doi:10.1371/journal.pone.0085165.t003

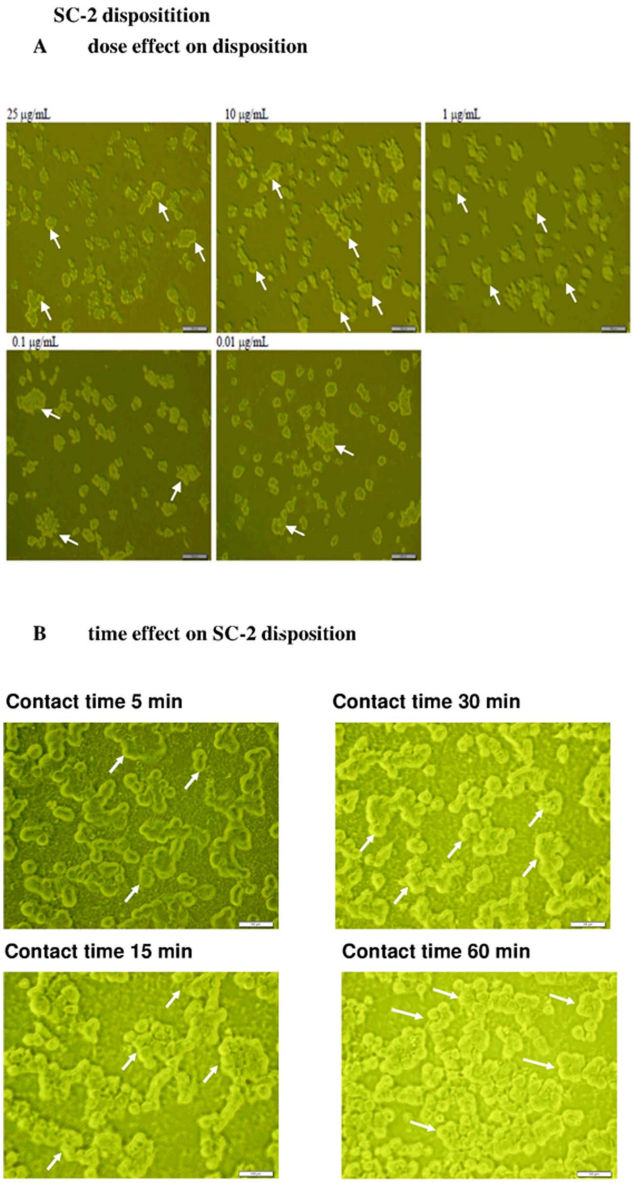

Figure 6. Fluorescent labeling technique to investigate the intracellular deposition of SC-2 into the HepG2 cells (×400). The dose effect (A), and the time effect (B). SC-2 was covalently labeled in equimolar ratio with FITC to form FITC-SC-2. In experiment A: Hep G2 cells at 1×10^5 cells/mL were seeded onto 3.5 cm plate containing 2 mL of DMEM and incubated for 24 h. FITC-SC-2 at 0.01, 0.1, 1.0, 10, and 25 μg/mL was added, and the incubation was continued for 30 min. In experiment B: Hep G2 cells at 1×10^5 cells/mL were seeded onto 3.5 cm plate containing 2 mL of DMEM and incubated for 24 h. FITC-SC-2 (10 μg/mL) was added, and the incubation was continued and sampled at the hour as indicated. As seen, in both experiments the FITC-SC-2 probes remained exclusively onto the outer membrane. Blank arrows indicate the non-fluorescent intracellular compartment.
doi:10.1371/journal.pone.0085165.g006

At 48 h, the respective killing capabilities were found to be 2.93×10^5 cells/mM, 1.46×10^5 cells/mM and 3.94×10^5 cells/mM when used alone. The combined use with SC-2 obviously altered the cytotoxic effects to 1.71×10^5 cells/mM, 1.73×10^5 cells/mM and 4.29×10^5 cells/mM, respectively for SB, and GmC and SA (Table 3). However at 72 h, the killing capabilities of free SB and free GmC were only comparable to those at 48 h. Conversely, SC-2 astonishingly significantly enhanced the cytotoxicity of GmC and SA to 3.94×10^5 cells/mM and 7.50×10^5 cells/mM, respectively (Table 3, Fig. 5A & 5B).

The SC-2 peptidoglycan was not transportable through the HepG2 cell membrane

SC-2 was totally nontoxic when used alone at a wide range of dosages (Fig. 5A), implying that free SC-2 was not mobilized into HepG2 cells. The florescent technology revealed the FITC-SC-2 molecules exclusively remained on the outer membrane of HepG2 cells even after 30 min of contact. No apparent difference was seen from the dose effect (Fig. 6A). However, the time-effect showed distinct higher accumulation of SC-2 on cell membrane (Fig. 6B).

TUNEL Assay

Free lignans were shown to be very effective in inducing apoptosis of HepG2 cells. DNA fragmentation was clearly perceivable by the TUNEL assay (Fig. 7A). In the presence of SC-2, the number of apoptotic cells was seen to have significantly increased (Fig. 7B).

Thermodynamic consideration of the transport process

To give a clear image of the role of SC-2 in the transport process for lignans, we proposed the diagrammatic model shown as Figure 8, which demonstrates the transport model of lignans through HepG2 cell membrane in the presence and absence of SC-2. It was assumed that the conformation of SC-2 was specifically altered when submerged onto the outer membrane of target cells, concomitantly, the free energy change declined to $\Delta G<0$. The membrane-bound SC-2 specifically accumulated the lignans and pumped them into the intramembraneous space. The cytosolic lignan concentration was thus rapidly raised to a higher level than the original extracellular concentration. Supposedly, GmC bearing an OH-group at position 7 (Fig. 1) could be more tightly arrested by SC-2. To quantify the magnitude of free energy changes, we defined two paths that transported lignans (Fig. 9), i.e. the path 1, in the absence of SC-2; and the path 2, in the presence of SC-2 In reality, path 1 is the common passive transport of lignans in the absence of SC-2. In path 1, the initial bulk fluid concentration of lignans (initial concentration C_0) was passively transported a distance of X_1 through the bulk fluid (reaction constant k_7) and the cell membrane (thickness X_2, reaction constants k_8) to reach the inner membrane where due the membrane barrier the concentration dropped sharply to the effective innermembraneous concentration C_{fl}, which was then moved into the cytoplasmic compartment and degraded (reaction constant k_9) to C_{mE} at the reaction site of intracellular compartment (Fig. 9). Path 2 is the SC-2-assisted transport in which lignans in the bulk fluid (concentration, C_0) were rapidly taken up by SC-2 already conjugated with the outer membrane (through a distance X_1, reaction constant k_4), where the outer membrane concentration rapidly dropped to C_{om}. Due to the "actively" pumping effect of SC-2, the intramembraneous lignan concentration was rapidly raised to C_{mA} (through a distance of membrane thickness X_2, reaction constant k_5), which, on moving along the inner membrane barrier, abruptly dropped down to C'_{mA} and simultaneously transferred into the cytoplasmic compartment and soon degraded to attain the final concentration C_{mE} at the reaction site (reaction constant k_6).

The elucidation for thermodynamic mathematical model is shown in Text S1. From the initial total extracellular concentrations and the extracellular and the intracellular concentrations at the pseudoequilibrium state (Table 2), the estimated parameters

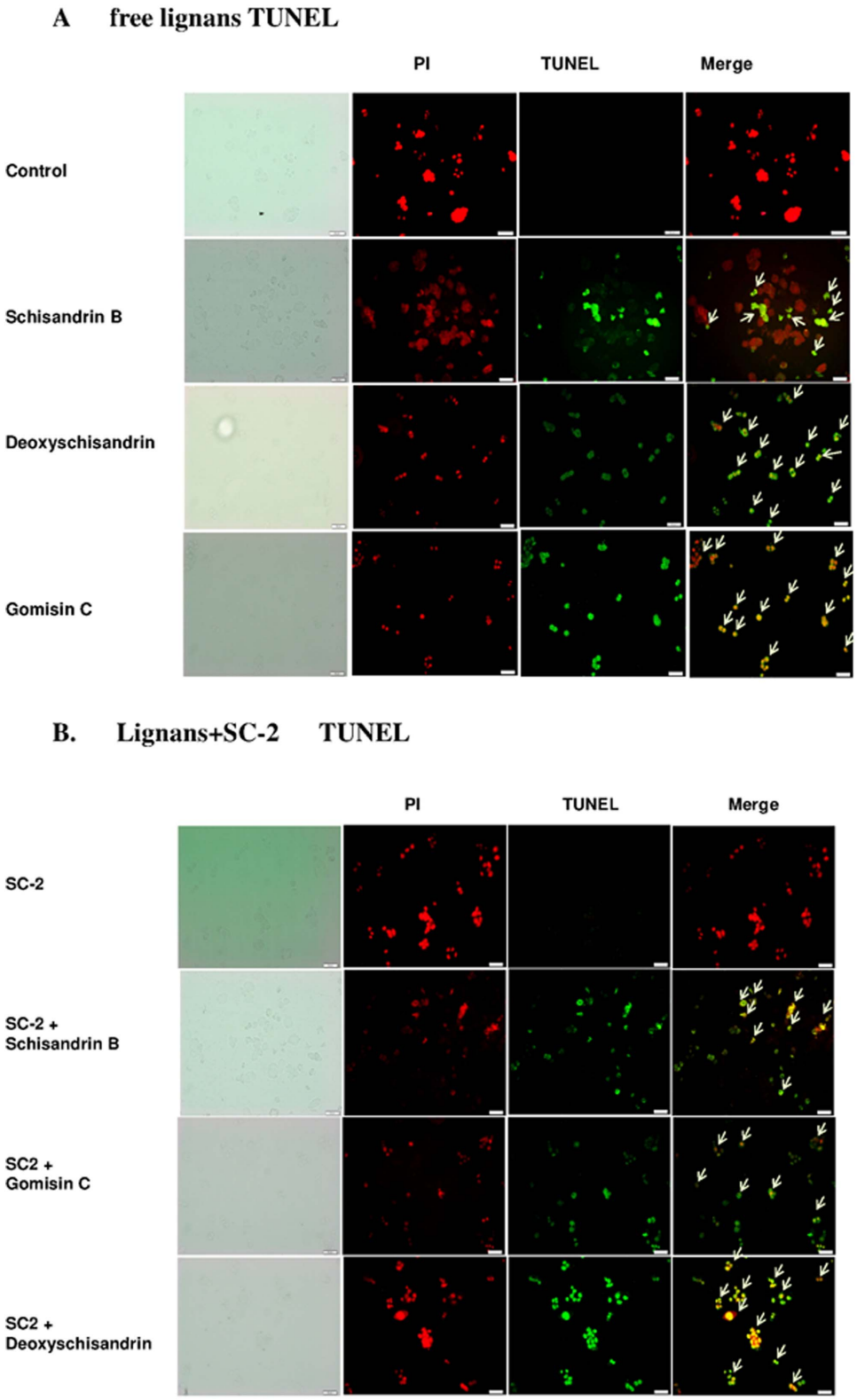

Figure 7. TUNEL assay for HepG2 cells. Cells treated with free lignans (A), and lignan plus SC-2 (B). Cells were induced for 24 h, then PI staining and TUNEL assay were carried out. Results were examined under a fluorescence microscope (×400).
doi:10.1371/journal.pone.0085165.g007

were obtained. The peak concentration was the highest for SB followed by GmC and SA (Table 4). By following the model presented in Figure 8 and Figure 9, the magnitude of the stepwise free energy change for each transport step was calculated (Table 5, see Text S1), from which the overall free energy change exampled by the largest ΔG_3 of SA (Table 2, Table 4) was achieved (Table 6).

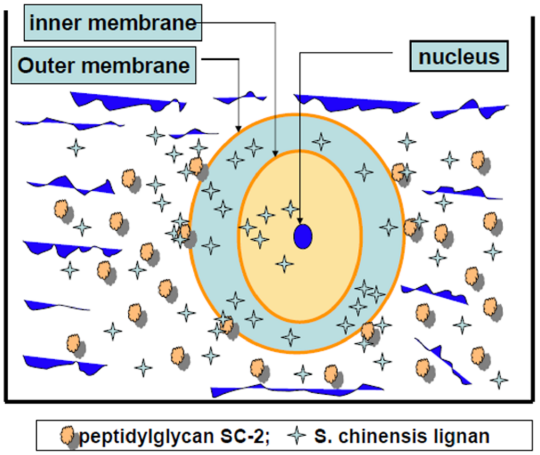

Figure 8. Diagrammatic model showing the transport of *S. chinensis* lignans through the HepG2 cell membrane in the presence and absence of peptidylglycan SC-2. The conformation of SC-2 was specifically altered when submerged onto the outer membrane of target cells, concomitantly, the free energy change declined to $\Delta G<0$. The membrane-bound SC-2 specifically accumulated the lignans and pumped them into the intramembrane space. The cytosolic lignan concentration was thus rapidly raised to a higher level than the original extracellular concentration. Supposedly, Gomisin C bearing an OH-group at position 7 (Fig. 1) could be more tightly arrested by SC-2.
doi:10.1371/journal.pone.0085165.g008

As can be expected, the other overall free energy changes would also remain at values of $\Delta G_{overall} = -\infty$ (Table 6).

Discussion

The powder XRD (Fig. 3D) revealed SC-2 to be high pure microcrystalline lattice structures with characteristic intra-lattice dimensions of $d_1 = 2.139$ Å, $d_2 = 1.786$ Å, and $d_3 = 1.300$ Å. Speculatively, the strongest diffraction of θ_3 could be due to diffraction from the main plane with alpha helical units lining up to elicit an inter-unit distance of 1.300 Å. While the other two distances, d_1 and d_2, may have been due to diffractions at secondary minor lattice planes. The specific molar extinction coefficients, the characteristic ratio of proteins to carbohydrates (= 0.4089) and the strong hydrogen bonding and amide absorption bands as well as the β-glycosidic linkage absorption bands at 768.66 cm^{-1} and 761.78 cm^{-1} ($\delta_{C\text{-}O}$, β-glycosidic linkage, w) evidenced the characteristic nature of a peptidoglycan (Fig. 3C). SC-2 was named 'rhamnofucosan' herein due to its unusual high fucose and rhamnose contents. The strong absorption at 280 nm implied the presence of huge amount of aromatic amino acids [32]. The exceptionally large amount of essential amino acid content (80.3%) implicated the traditional medicinal use of SC-2 as a hepatoprotective agent (attributed to cysteine and methionine) and the building blocks for the active sites or signaling sites (usually contributed by tyrosine, cysteine, and histidine) [33] (Table 1).

On the other hand, the apparently perceivable difference in FTIR absorption spectra GmC, SB and SA could be due to the exocyclic methylene between C12 and C13 in both SB and GmC and the benzoyl ester at C6 of GmC. Similar results were reported by Ma et al. [34]. To our astonishment, the FTIR spectra of the pure SC-2 (Fig. 3C) and the lignan+SC-2 appeared extremely alike (Figs. 4A–4C, lower panels), underlying the occurrence of strong intermolecular interaction between lignans and SC-2 due to complete entrapment of lignans into SC-2 macromolecule.

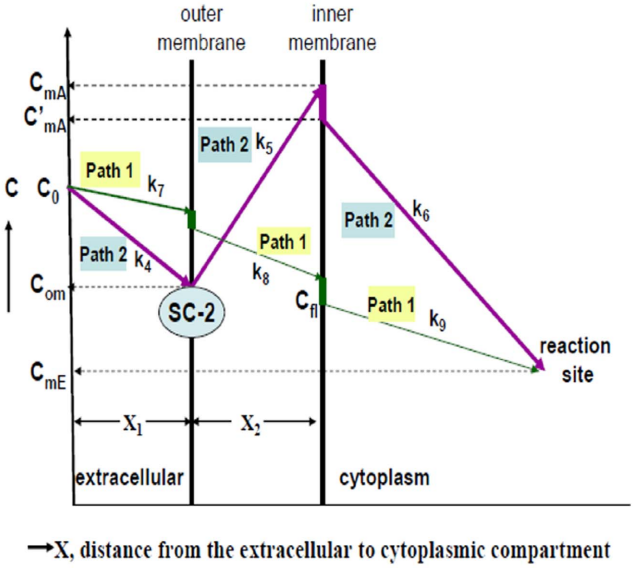

Figure 9. Two different transport mechanisms with detailed concentration changes along the paths. In path 1, the initial bulk fluid concentration of lignans (initial concentration C_0) was passively transported a distance of X_1 through the bulk fluid (reaction constant k_7) and the cell membrane (thickness X_2, reaction constants k_8) to reach the inner membrane where due the membrane barrier the concentration dropped sharply to the effective innermembraneous concentration C_{fl}, which was then moved into the cytoplasmic compartment and degraded (reaction constant k_9) to C_{mE} at the reaction site of intracellular compartment (Fig. 9). Path 2 is the SC-2-assisted transport in which lignans in the bulk fluid (concentration, C_0) were rapidly taken up by SC-2 already conjugated with the outer membrane (through a distance X_1, reaction constant k_4), where the outer membrane concentration rapidly dropped to C_{om}. Due to the "actively" pumping effect of SC-2, the intramembrane lignan concentration was rapidly raised to C_{mA} (through a distance of membrane thickness X_2, reaction constant k_5), which, on moving along the inner membrane barrier, abruptly dropped down to C'_{mA} and simultaneously transferred into the cytoplamic compartment and soon degraded to attain the final concentration C_{mE} at the reaction site (reaction constant k_6).
doi:10.1371/journal.pone.0085165.g009

Biologically, SC-2 was entirely non-cytotoxic, while the slight decline in viability found for doses ≥800 μgmL^{-1} could have been due to the membrane-masking or -plugging exerted by SC-2 (Fig. 5, right lower panel).

Pharmacokinetically, the uptake rates of both SB and SA were apparently enhanced, conversely, GmC significantly retarded by SC-2 (Table 2). To interpret this, we assumed that the uptake of lignans obeyed first-order kinetics with respect to the free *Schisandra* lignan when used alone (eq. 1), whereas it obeyed a second-order kinetic in the presence of SC-2 (eq. 2):

$$d[C]/dt = k_1[C] \quad (1)$$

and

$$d[C]/dt = k_2[C][S] \quad (2)$$

where C is the concentration of SC lignans ($\mu mol\ L^{-1}$), t is the duration of incubation time (min), and S is the amount of SC-2 present in the reaction mixture (herein SC-2 = 1 $mgmL^{-1}$ or 1.1891 $\mu mol\ L^{-1}$). The parameters k_1 and k_2 are first- and the second-order uptake rate coefficients, respectively. The calculated uptake kinetic parameters are listed in Table 2. As shown, in the

Table 4. Estimation of the parameters at status of pseudo equilibrium.

Parameter	Initial totalextracellular concentration	Extracellular concentration (mM)	Intracellularconcentration, Ls_{in} (mM)
[SC-2][a]	1 mg/mL (1.1891×10^{-3} mM)	0.0	0.0
[M_{outer}]	[M_{outer}]>>[SC-2], hence [M_{outer}]	[M_{outer}]>>[SC-2], hence [M_{outer}]	-
	≈constant	≈constant	
[SC-2-M_{outer}]	1.1891×10^{-3} mM	1.1891×10^{-3} mM	0.0
Ls[c]:	$C_0 = 0.1$ mM	-	(peak concentration)[c]
Schisandrin B	$C_0 = 0.1$ mM	$C_{0m} = 0.007$ mM	$C_{mA}' = 0.093$ mM;
Gomisin C	$C_0 = 0.1$ mM	$C_{0m} = 0.081$ mM	$C_{mA}' = 0.019$ mM;
Deoxyschsandrin	$C_0 = 0.1$ mM	$C_{0m} = 0.085$ mM	$C_{mA}' = 0.015$ mM;
			Assume C_{mA}'
			≈C_{mA}(Fig. 8)
[SC-2-M_{outer}]-Ls	1.1891×10^{-3} mM	1.1891×10^{-3} mM	0.0
C_{mE}[b,c]:	-	-	-
Schisandrin B	-	-	0.005 mM
Gomisin C	-	-	0.005 mM
Deoxyschsandrin	-	-	0.005 mM

[a]SC-2: MW = 841 kDa. 1 mg/mL = 1.1891×10^{-3} mM.
[b]C_{mE}: estimated from Fig. 9.
[c]Be referred to Text S1, Table 2 and Fig. 9.
doi:10.1371/journal.pone.0085165.t004

Table 5. Magnitude of parameters related with the free energy changes during the transport of lignans in the absence or presence of SC-2.

Parameters	Values of change in free energy, kcal/mol			
	$\Delta G_{0,1}$	$\Delta G_{0,2}$	$\Delta G_{0,3}$	$\Delta G_{0,4}$
[SC-2][a]	≈0.0	-	-	-
[M_{outer}][b]	Constant K	-	-	-
[SC-2-M_{outer}], M	$\approx1.1891\times10^{-6}$	$\approx1.1891\times10^{-6}$	-	-
[Ls], M	-	9.988×10^{-4}		
[SC-2-M_{outer}]-Ls, M		$\approx1.1891\times10^{-6}$	$\approx1.1891\times10^{-6}$	
[Ls_{in}][c], M	-	-	-	-
Schisandrin B	-	-	46×10^{-6}	46×10^{-6}
Gomisin C	-	-	10×10^{-6}	10×10^{-6}
Deoxyschisandrin	-	-	55×10^{-6}	55×10^{-6}
C_{om}, M	-	-	-	-
Schisandrin B			$C_{0m} = 7\times10^{-6}$	
Gomisin C			$C_{0m} = 81\times10^{-6}$	
Deoxyschsandrin			$C_{0m} = 85\times10^{-6}$	
C_{mA}', M	-	-	-	
Schisandrin B			$C_{mA}' = 93\times10^{-6}$;	
Gomisin C			$C_{mA}' = 19\times10^{-6}$;	
Deoxyschsandrin			$C_{mA}' = 15\times10^{-6}$	
C_{mE}[d], M	-	-	-	-
Schisandrin B				5×10^{-6}
Gomisin C				5×10^{-6}
Deoxyschsandrin				5×10^{-6}

[a]SC-2: MW = 841 kDa. 1 mg/mL = 1.1891×10^{-6}M.
[b]The concentration of SC-2 was very small compared to that of outer membrane, hence [M_{outer}] was considered to be constant and designated K.
[c]Values obtained by extrapolation to zero time zero.
[d]C_{mE}: estimated from Fig. 6.
doi:10.1371/journal.pone.0085165.t005

Table 6. The overall free energy changes during the transport of *S. chinensislignans* from the extracellular into the intracellular compartment[a].

Parameters				
	$\Delta G_{0,1}$	$\Delta G_{0,2}$	$\Delta G_{0,3}$	$\Delta G_{0,4}$
Free energy changes, KJ	$-\infty$	−2.572	+0.059[c]	$-\infty$
K_{eq}, mol^{-1}	$K_{eq'} = K_{eq} \times K = +\infty$[b]	0.9980	−0.0189	$+\infty$[d]
Equation applied	Eq. 3–Eq. 6	Eq. 7–Eq. 9	Eq. 11, Eq. 12	Eq. 13–Eq. 16
Overall free energy change = $\Delta G_{0,1}+\Delta G_{0,2}+\Delta G_{0,3}+\Delta G_{0,4} = -\infty$				

[a]Free energy changes = $-RT\ell nK_{eq}$(J). R = 8.314 JK^{-1} mol^{-1}. T = 310 K.
[b]$K_{eq'}$ is a pseudoequilibrium constant. K is the amount of outer membrane concentration defined in Table 5.
[c]Value of ΔG_3 was exampled by the largest value (of deoxyschisandrin) among these three lignans (be referred to Table 2).
[d]The value K_{eq} in calculation of $\Delta G_{0,4}$ in reality is not an equilibrium constant because reversible reaction does not occur in the intracellular degradation process. The value was estimated by the difference between the initial and the final conditions (be referred to text).
doi:10.1371/journal.pone.0085165.t006

presence of SC-2, the initial uptake rate constants (in $L{\bullet}mmol^{-1}$ - min^{-1}) for SB, GmC and SA were 2.016×10^{-5}, 5.046×10^{-6}, and 1.264×10^{-5}, respectively. A similar trend was also perceivable in free lignans but to a lesser extent (Table 2).

Worth noting, free SA uniquely revealed a relatively delayed uptake rate compared to those of GmC and SA. Intracellular concentrations of GmC were rapidly consumed up at 30 min for GmC and at 60 min for SA, both similarly yielding intracellular decay rates -1.092×10^{-6} $L{\bullet}mmol^{-1}$ min^{-1} (Table 2), as contrast, the uptake of SB required much longer time. While in the presence of SC-2, the uptake of GmC was significantly suppressed (Table 2). The reason could be attributed to the retardation effect of SC-2 on the benzoyl esteric and C7-OH of GmC (Fig. 1). Over time, the total delivery rates became with the order SB>SA>GmC. Speculatively, the therapeutic indication of whole SC would be mostly depending on SB (Table 2).

Pharmacodynamically, the improved IC_{50} values in time- and dose-dependent manner apparently implied that the enhanced transport of SB (gomisin N) and GmC had been affected by SC-2 (Table 3, Fig. 5A & 5B). A previous report indicated the respective IC_{50} values to be 0.043 and 0.336 mM with respect to human colorectal cancer cell line HT-29 [35]. As contrast, the IC_{50} values for HepG2 cells were 0.19 mM for free SA and 0.15 mM for combined SA with SC-2, indicating cell-specific drug-susceptibilities.

Now the question arises: How did SC-2 affect the pharmacokinetic and pharmacodynamic outcomes of SC-lignans? To solve this issue, the FITC fluorescence technique was applied. Amazingly, labeled SC-2 was shown to have been completely unmobilized into the cell membrane (Fig. 6A & 6B).

As was described in ''Materials and methods'', FITC-SC-2 was added at 0.01, 0.1, 1.0, 10.0, and 25 μgmL^{-1}, which respectively corresponded to final concentrations of 0.0025 to 6.25 μgmL^{-1}. These amounts elicited approximate coverage rates (number of fmoles of FITC-SC-2 per HepG2 cell) of 3.0×10^{-5} to 7.5×10^{-2} fmoles $cell^{-1}$. Taking the Avogadro's number (6.02×10^{23} molecules/mole) into account, the respective coverage rates became 1.81×10^{4} to 4.52×10^{7} FITC-SC-2 particles/cell, underlying the fuzzy appearance (Fig. 6B). Thus, in order to obtain a clearer image, we adopted concentrations much lower than those used for the MTT assay (Figs. 5A, Fig. 6A, 6B). More importantly, results distinctly revealed SC-2 molecules to be preferentially adhered onto the outer membranes of HepG2 cells (Fig. 6A, 6B), consistent with the widely cited [36,37]. Literature elsewhere indicated that SA with two methoxy groups respectively located at positions C12 and C13 (Fig. 1) could show the most cytotoxic behavior (i.e. the lowest IC_{50} value) compared to GmC and SB (Gomisin N) [37,38] (Table 3). The latter two compounds exhibit an exocyclic methylene (-O-CH_2-O-) linkage instead of two methoxy groups (Fig. 1) [36,37], indicating exocyclic methylene linking C12 and C13 to be cytotoxicity attenuation-related. Supposedly, the C12 and C13 methoxy groups hindered the SA transport. Conversely, the exocyclic methylene (-O-CH_2-O-) linkage favored the rapid transport of SB and GmC (Table 2). Strong bioactivity can be attained by lignans structurally without ester group at C-6 and a hydroxyl group at C-7 or an exocyclic methylene chain between C12 and C13, but with an R-biphenyl configuration (Fig. 1, Table 3) [37]. Worth noting, 6(7)-dehydroschisandrol A, a derivative of SA, showed the highest activity (IC_{50}, 2.1 μM) as a platelet-activating factor antagonist [38].

SB (Gomisin N) was shown to increase the resistance of mitochondria to calcium ion-induced disruption, effectively preventing the apoptosis of hepatic cells under stressful conditions [39,40].

TUNEL assay indicated the approximate order of cytotoxicity to be: SA>SB>GmC (Fig. 7A). All the combined therapies elicited rather large extents of apoptosis (Fig. 7B). Interestingly, when treated with combined SC-2 the order of cytotoxicity changed to SC-2+SA>SC-2+GmC>SC-2+SB, consistent with the MTT assay (Table 3).

Now, the question arises ''Could such non-spontaneous unidirectional transport be allowed to occur?'' To resolve this problem, we performed a theoretical calculation using the Second Law of Thermodynamics (please be referred to Text S1) (Table 4, Table 5). Results in Table 6 indeed evidenced such a ''Catcher-Pitcher Unidirectional Transport Mechanism'' (Fig. 8, Fig. 9).

Finally, SC-2 exhibited appreciable water solubility (unpublished), implying that the feasible role of decoction in Traditional Chinese Medicinal preparations.

Conclusions

The pure peptidoglycan SC-2 obtained from *S. chinensis* fruits is nontoxic to the HepG2 cell line. SC-2 increases the transport and cytotoxicity of SC lignans by the ''Catcher-Pitcher Unidirectional Transport Mechanism'', underlying the beneficial effect of SC-2 to improve the hepatoprotective effect. Physical chemically, the Second Law of Thermodynamics allows such a unidirectional transport phenomenon. More importantly, the pharmacodynamic behavior greatly improved by the combined therapy (SC-2+lignans) implies the decoction philosophy for preparation of the Traditional Chinese Medicine.

Supporting Information

Figure S1 HPLC, UV-Visible, ESI-MS and ESI-MS-MS analyses (top to bottom) of dibenzocyclooctadiene lignans isolated from *S. chinensis* fruits. Gomisin C (GmC); deoxyschisandrin (SA); schisandrin B (SB). The molecular weights: gomisin C, 536.6; deoxyschisandrin, 416.5; and schisandrin B, 400.5, respectively.
(TIF)

Text S1
(DOC)

Author Contributions

Conceived and designed the experiments: CCP RYP. Performed the experiments: CCC. Analyzed the data: YBK SHH. Contributed reagents/materials/analysis tools: CHC HEW. Wrote the paper: CCC RYP.

References

1. Day AJ, Prestwich GD (2002) Hyaluronan-binding proteins: tying up the giant. J Biol Chem 277:4585–4588.
2. Toole BP (2004) Hyaluronan: from extracellular glue to pericellular cue. Nat Rev Cancer 4: 528–539.
3. Janes KA, Calvo P, Alonso MJ (2001) Polysaccharide colloidal particles as delivery systems for macromolecules. Adv Drub Rev 47: 83–97.
4. Liu M, Wu K, Mao X, Wu Y, Ouyang J (2010) Astragalus polysaccharide improves insulin sensitivity in KKAy mice: regulation of PKB/GLUT4 signaling in skeletal muscle. J Ethnopharmacl 127: 32–37.
5. Shihorka V, Vyas SP (2001) Potential of polysaccharide anchored liposomes in drug delivery, targeting and immunization. J Pharm Pharmaceut Sci 4: 138–158.
6. Polyakov NE, Leshina TV, Meteleva ES, Dushkin AV, Konovalova TA, et al. (2010) Kispert LD. Water soluble carotenoid conjugates with oligo- and polysaccharides synergy of drug transport and efficacy. NSTI Nanotech 3: 312–315.
7. Victor R, Chauzy C, Girard N, Gioanni J, d'Anjou J, et al. (1999) Human breast-cancer metastasis formation in a nude-mouse model: studies of hyaluronidase, hyaluronan and hyaluronan-binding sites in metastatic cells. Int J Cancer 82: 77–83.
8. Kuang DM, Wu Y, Chen N, Cheng J, Zhuang SM, et al. (2007) Tumor-derived hyaluronan induces formation of immunosuppressive macrophages through transient early activation of monocytes. Blood 110: 587–595.
9. Yim SY, Lee YJ, Lee YK, Jung SE, Kim JH, et al. (2009) Gomisin N isolated from *Schisandra chinensis* significantly induced anti-proliferative and pro-apoptotic effects in hepatic carcinoma. Mol Med Rep 2: 725–732.
10. Ip SP, Mak DH, Li PC, Poon MK, Ko KM (1996) Effect of a lignan-enriched extract of *Schisandra chinensis* on aflatoxin B1 and cadmium chloride-induced hepatotoxicity in rats. Pharmacol Toxicol 78: 413–416.
11. Cyong JC, Ki SM, Lijima K, Kobayashi T, Furuya M (2000) Clinical and pharmacological studies on liver diseases treated with Kampo herbal medicine. Am J Chin Med 28: 351–360.
12. Lu Y, Chen DF (2009) Analysis of *Schisandra chinensis* and *Schisandra sphenanthera*. J Chromatogra A 1216: 1980–1990.
13. Yin FZ, Yin W, Zhang X, Lu TL, Cai BC (2010) Development of an HPLC fingerprint for quality control and species differentiation of *Fructus schisandrae*. Acta Chromatogrphica 22: 609–621.
14. Xie Y, Hao H, Kang A, Liang Y, Xie T, et al. (2010) Integral pharmacokinetics of multiple lignan components in normal, CCl_4-induced hepatic injury and hepatoprotective agents pretreated rats and correlations with hepatic injury biomarkers. J Ethnopharmacol 131: 290–299.
15. Kim SR, Lee MK, Koo KA, Kim SH, Sung SH, et al. (2004) Dibenzocyclooctadiene lignans from *Schisandra chinensis* protect primary cultures of rat cortical cells from glutamate-induced toxicity. J Neurosci Res 76: 397–405.
16. Min HY, Park EJ, Hong JY, Kang YJ, Kim SJ, et al. (2008) Antiproliferative effects of dibenzocyclooctadiene lignans isolated from *Schisandra chinensis* in human cancer cells. Bioorg. Med Chem Lett 18: 523–526.
17. Fujihashi T, Hara H, Sakata T, Mori K, Higuchi H, et al. (1995) Anti-human immunodeficiency virus (HIV) activities of halogenated gomisin J derivatives, new nonnucleoside inhibitors of HIV type 1 reverse transcriptase. Antimicrob Agents Chemother 39: 2000–2007.
18. Ip SP, Ma CY, Che CT, Ko KM (1997) Methylenedioxy group as determinant of schisandrin in enhancing hepatic mitochondrial glutathione in carbon tetrachloride-intoxicated mice. Biochem Pharmacol 54: 317–319.
19. Oh SY, Kim YH, Bae DS, Um BH, Pan CH, et al. (2010) Anti-inflammatory effects of gomisin N, gomisin J, and schisandra C isolated from the fruit of *Schisandra chinensis*. Biosci Biotechnol Biochem 74: 285–291.
20. Zhu M, Yeung RY, Lin KF, Li RC (2000) Improvement of phase I drug metabolism with *Schisandra chinensis* against CCl_4 hepatotoxicity in a rat model. Planta Medica 66: 521–525.
21. Chang CY, Chen YL, Yang SC, Huang GC, Tsi D, et al. (2009) Effect of schisandrin B and sesamin mixture on CCl(4)-induced hepatic oxidative stress in rats. Phytother Res 23: 251–256.
22. Chen Y, Tang J, Wang X, Sun F, Liang S (2012) An immunostimulatory polysaccharide (SCP-IIa) from the fruit of *Schisandra chinensis* (Turcz.) Baill. Int J Biol Macromol 50: 844–848.
23. Yan F, Zhang QY, Jiao L, Han T, Zhang H, et al. (2009) Synergistic hepatoprotective effect of Schisandrae lignans with Astragalus polysaccharides on chronic liver injury in rats. Phytomed 16: 805–813.
24. La Torre GL, Saitta M, Vilasi F, Pellicano T, Dugo G (2006) Direct determination of phenolic compounds in Sicilian wines by liquid chromatography with PDA and MS detection. Food Chem 94: 640–650.
25. Ker YB, Chen KC, Chyau CC, Chen CC, Guo JH, et al. (2005) Antioxidant capability of polysaccharides fractionated from submerge-cultured *Agaricus blazei* mycelia. J Agric Food Chem 53: 7052–7058.
26. Dubois M, Gilles KA, Hamilton JK, Reders PA, Smith F (1956) Colorimetric method for determination of sugars and related substances. Anal Chem 28: 350–356.
27. Peng CH, Chang CH, Peng RY, Chyau CC (2010) Improved membrane transport of astaxanthine by liposomal encapsulation. Eur J Pharm Biopharm 75: 154–161.
28. Kanebo Y, Ueno T, Tanaka T, Iwase H, Yamaguchi Y, et al. (2000) Pharmacokinetics and biodisposition of fluorescein labeled arabinogalactan in rats. Int J Pharmaceut 201: 59–69.
29. Tanaka T, Fujishima Y, Hanano S, Kaneo Y (2004) Intracellular disposition of polysaccharides in rat liver parenchymal and nonparenchymal cells. Int J Pharmaceut 286: 9–17.
30. Borisov AB, Calson BM (2000) Cell death in denervated skeletal muscle is distinct from classical apoptosis. Anatom Rec 58: 305–318.
31. Gavrieli Y, Sherman Y, Ben-Sasson SA (1992) Identification of programmed cell death in situ via specific labeling of nuclear DNA fragmentation. J Cell Biol 119: 493–501.
32. Bradford MM (1976) A rapid and sensitive method for the quantitation of microgram quantities of protein utilizing the principle of protein-dye binding. Anal Biochem 72: 248–254.
33. Wetlaufer DB (1962) Ultraviolet spectra of proteins and amino acids. Adv Protein Chem 17: 303–390.
34. Ma WH, Lu Y, Huang H, Zhou P, Chen DF (2009) Schisanwilsonins A–G and related anti-HBV lignans from the fruits. Bioorg. Med Chem Lett 19: 4958–4962.
35. Gnabre J, Unlu I, Chang TC, Lisseck P, Bourne B, et al. (2010) Isolation of lignans from *Schisandra chinesis* with anti-proliferative activity in human colorectal carcinoma: Structure-activity relationships. J Chromatogr B 878: 2693–2700.
36. Opletal L, Krenkov??? M, Havl???ckov??? P (2010) Phytotherapeutic aspects of diseases of the circulatory system. 7. *Schisandra chinensis* (Turcz.) Baill.): its composition and biological activity. Ceska Slov Farm 50: 173–180.
37. Opletal L, Krenkov??? M, Havl???ckov??? P (2010) Phytotherapeutic aspects of diseases of the circulatory system. 8. Chinese magnolia (*Schisandra chinensis* (Turcz.) Baill.): production of the drugs and their evaluation, therapeutic and dietary preparations. Ceska Slov Farm 50: 219–224.
38. Lee IS, Jung KY, Oh SR, Park SH, Ahn KS, et al. (1999) Structure-activity relationships of lignans from *Schisandra chinensis* as platelet activating factor antagonists. Biol Pharm Bull 22: 265–267.
39. Chiu PY, Leung HY, Siu AH, Poon MK, Ko KM (2007) Schisandrin B decreases the sensitivity of mitochondria to calcium ion-induced permeability transition and protects against carbon tetrachloride toxicity in mouse livers. Biol Pharm Bull 30: 1108–1112.
40. Iwata H, Tezuka Y, Kadota S, Hiratsuka A, Watabe T (2004) Identification and characterization of potent CYP3A4 inhibitors in Schisandra fruit extract. Drug Metab Dispos 32: 1351–1358.